IEEE Photonics Journal
An IEEE Photonics Society Publication

Open Access

All Polarization-Maintaining Passively Mode-Locked Yb-Doped Fiber Laser: Pulse Compression Using an Anomalous Polarization-Maintaining Photonic Crystal Fiber

(Invited Paper)

Volume 11, Number 6, December 2019

Christian Cuadrado-Laborde
Antonio Carrascosa
Antonio Diez
Jose L. Cruz
Miguel V. Andrés

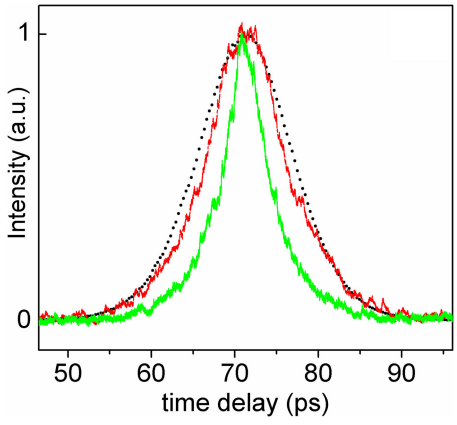

DOI: 10.1109/JPHOT.2019.2943839

IEEE photonics SOCIETY
IEEE

All Polarization-Maintaining Passively Mode-Locked Yb-Doped Fiber Laser: Pulse Compression Using an Anomalous Polarization-Maintaining Photonic Crystal Fiber

(Invited Paper)

Christian Cuadrado-Laborde [1,2,3] **Antonio Carrascosa,** [1] **Antonio Diez** [1] **Jose L. Cruz** [1] **and Miguel V. Andrés** [1]

[1]Departamento de Física Aplicada, ICMUV, Universidad de Valencia, E-46100 Burjassot, Spain
[2]Instituto de Física Rosario (CONICET-UNR), S2000EZP Rosario, Argentina
[3]Facultad de Química e Ingeniería, Pontificia Universidad Católica Argentina, 2000 Rosario, Argentina

DOI:10.1109/JPHOT.2019.2943839
This work is licensed under a Creative Commons Attribution 4.0 License. For more information, see https://creativecommons.org/licenses/by/4.0/

Manuscript received June 4, 2019; revised September 18, 2019; accepted September 21, 2019. Date of publication September 25, 2019; date of current version November 20, 2019. This work was supported by the Agencia Estatal de Investigación of Spain and Fondo Europeo de Desarrollo Regional (Ref.: TEC2016-76664-C2-1-R). The work of C. Cuadrado-Laborde was supported by the Project PICT 2015-1828 (FONCYT, Argentina), in part by PIP 11220150100607CO (CONICET, Argentina), and in part by the Programa de Investigadores Invitados de la Universidad de Valencia (Spain) (Ref.: UV-INV-EPC18). Corresponding author: Christian Cuadrado-Laborde (e-mail: christian.cuadrado@uv.es).

Abstract: We report the generation of short pulses at 1 μm using an all-polarization-maintaining (PM) fiber configuration. The pulses are provided by an all normal-dispersion Fabry-Perot Yb-doped cavity and are compressed with an anomalous polarization-maintaining photonic crystal fiber (PM PCF). Opposed to standard configurations; here the filtering action is solely performed by the finite bandwidth of the gain medium. The laser generates 8 ps width sech^2 profile pulses at 1046.8 nm with a -10 dB bandwidth of 5.9 nm. After compression using the PM PCF, pulses with an FWHM of 3 ps were obtained, limited by the actual value of the available anomalous dispersion. We also report the changes in the output light pulses when both the net-normal dispersion of the cavity and the medium gain length were varied. We found that the lack of a specific filter within the cavity does not deteriorate the performance as compared with previous works.

Index Terms: Fiber laser, dissipative solitons, polarization maintaining, photonic crystal fibers.

1. Introduction

Soliton mode-locking is the route originally taken towards the generation of short light pulses [1], [2]. However, it is necessary a precise balance between chromatic dispersion and nonlinearity that unfailingly requires anomalous chromatic dispersion, which is otherwise easily attainable at 1.5 μm. However, at 1 μm, conventional single-mode fibers and fiber components have normal

dispersion; notwithstanding that soliton mode-locking is still possible by including into the cavity a dispersion-compensator—e.g.,: free-air grating-pairs photonic crystal fibers, etc.—which shift the chromatic dispersion from normal to net-anomalous, but at the expenses of higher power loses. Additionally, the performance of soliton mode-locked fiber lasers is very limited, where picojoules energies are typical for picosecond pulse durations; not to mention the technical difficulties associated with the operation of these lasers generally slightly above the lasing threshold to avoid multi-pulsing. It is also possible to take a different route towards short pulse generation at 1 μm; i.e., by using dissipative optical solitons. Dissipative optical solitons in a nonlinear medium are confined wave packets of light whose existence and stability depend essentially on the energy balance [3]. Although the first contributions of dissipative optical solitons were first studied in nonlinear optics, it turned out this new concept was sufficiently general to be applied to other research areas. In this work we will refer specifically to DSs generated in all-normal-dispersion (ANDi) cavities. In this case, and in contrast to solitons—which are Fourier-transform-limited—; DSs are positively chirped pulses, which can be recompressed outside the cavity into the ultrashort regime [4], [5]. DSs are solutions of the cubic complex Ginzburg-Landau equation; when compared with standard solitons, DSs offer higher energies and stability, avoiding the challenge to provide low-loss net-anomalous dispersion at 1 μm.

ANDi fiber lasers able to deliver—after out-of-cavity recompression—ultrashort light pulses in the tens of femtoseconds have been reported [4], [5]. However, they were not strictly all-fiber lasers, since free-space components were used, therefore suppressing the benefits offered by a full waveguide medium. Strictly all in-fiber ANDi lasers were also presented, nonetheless relying on nonlinear polarization evolution, which can hardly be compatible with an all-polarization maintaining (PM) cavity [6], [7]. An all in-fiber PM solution is highly desirable because ensures the environmental robustness required for out-of-laboratory applications [8]. Recently, different ANDi PM fiber lasers were presented [9]–[17] having all in common the use of a strong filtering within the cavity by using: a bandpass pigtailed PM filter with 1.7 to 2.8 nm-bandwidth [9], [11], [13]–[17], tilted fiber Bragg gratings with 14–17 nm bandwidth [10], and chirped fiber Bragg grating with 16 nm bandwidth [12]. This is because it has been recognized before that DSs pulse shaping in ANDi lasers is based on spectral filtering of the chirped pulse, which cuts off the temporal wings of the pulse after each round-trip [18]. Examples in the literature without a specific filter in an ANDi PM Yb-doped fiber laser are scarce, and with output light pulses well in the nanoseconds range [19]. Here we give one step forward in the simplification of ANDi PM fiber lasers, by studying its behavior when the filtering action is solely performed from the intrinsic finite gain bandwidth of the active fiber. This simplified all-in-fiber PM ANDi Yb-doped laser was characterized in detail, and later we analyzed its potential for out-of-cavity recompression. Next, we also measured the changes in the output light pulses when the net-normal dispersion of the cavity and the medium gain length were varied.

2. Experimental Details

A schematic diagram of the mode-locked laser is illustrated in Fig. 1; the laser operates in a Fabry-Pérot configuration. The gain was provided by a PM ytterbium highly-doped, single-clad, optical fiber (PM YDF) (YDF-SM-6/125 panda clad shape by NOVAE, core absorption $>$700 dB/m at 975 nm, and a numerical aperture of 0.16 $\pm$ 0.02). The PM YDF was pumped through a PM wavelength division multiplexer (PM WDM, 980 nm/1060 nm) by a 976 nm emission wavelength pigtailed laser diode, providing a maximum pump power of 500 mW. Next, the PM YDF was spliced to the input port of an 80/20 PM fiber coupler (PM OFC, slow axis working and fast axis blocked). The 80% port of the PM OFC was in turn spliced to the SESAM (Batop GmbH, high reflection band 1010 nm $\leq \lambda \leq$ 1110 nm, relaxation time constant 1 ps). The cavity was closed by connecting the remaining port of the PM WDM to a PM fiber-pigtailed dichroic mirror (80% reflectivity at 1030 nm). In some experiments, it was also included a delay line, between the PM YDF and the input of the PM OFC. Finally, the output of this laser is obtained through the 20% port of the PM OFC, where a fiber pigtailed polarization-maintaining optical isolator was also included in order to avoid unwanted reflections to the cavity. We emphasize the complete lack of a filter within the cavity. The filtering performance of the different components within the cavity should not be taken into account due to

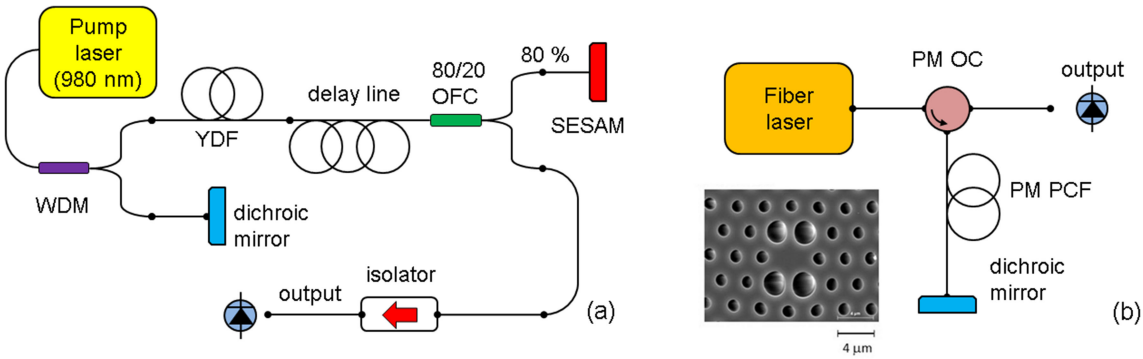

Fig. 1. (a) Experimental laser setup. (b) Experimental setup for out-of-cavity recompression; the photograph is a scanning electron microscope image of a transversal slide of the PM PCF.

its broadband characteristics; as an example, the measured −3 dB bandwidth of the PM OFC is 69 nm.

The original configuration had no delay line and a PM YDF length of 0.39 m; this configuration of the cavity includes the pigtails of the polarization-maintaining fiber optics components (WDM, OFC, etc.), which all have normal dispersion, limiting in this way the round-trip cavity length to 4.23 m. We also investigated the behavior of our laser by adding a delay line, which was made of different lengths of a PM single-mode fiber (PM SMF) (PM980-XP by Nufern, a cut-off wavelength of 920 ± 50 nm, and a numerical aperture of 0.120), to the original configuration, see Fig. 1(a). The presence of the delay line allows changing the net (normal) dispersion of the cavity. Our study begins with a full characterization of the original configuration. Next, we investigated the possibility to recompress the output light pulses provided by this laser, by further propagation through an anomalous dispersive line −out of the resonant cavity, made of a polarization-maintaining photonic crystal fiber (PM PCF) fabricated in our facilities. We also studied how the output light pulse provided by this laser changes under a variation in the PM YDF length, by using PM YDF lengths of 0.13 m, 0.2 m, 0.25 m, 0.31 m, 0.36 m, 0.39 m (original configuration) and 0.5 m. Finally, we analyzed the effect of dispersion on the output light pulses, by progressively increasing the net (normal) dispersion within the cavity, with the addition of PM SMF with lengths of 3.75 m, 3.97 m, 4.88 m, 6.55 m and 9.6 m; whereas the PM YDF length remained simultaneously fixed to 0.5 m. Figure 1(b) shows the experimental setup for pulse compression; the presence of the polarization-maintaining optical circulator (PM OC) and the dichroic mirror (80% transmissivity), allows us to simultaneously testing single and double passes through the PM PCF. On the other hand, the inset in Fig. 1(b) shows a photograph obtained with a scanning electron microscopy of the transversal slide of the PM PCF used in the compression experiments; the strong geometrical anisotropy observed is ultimately responsible for the polarization preservation.

We measured in our laboratory by the interferometric technique the dispersions of the PM SMF and the PM PCF resulting in 24 ps^2/km, and −9 ps^2/km, respectively, at 1030 nm; whereas we estimated the dispersion of the PM YDF to be 25 ps^2/km. Therefore, the net (normal) dispersion of the original configuration was 0.107 ps^2 (the dispersion of the SESAM can be neglected since averages zero around 1040 nm). On the other hand, when the PM YDF length was changed, the net (normal) dispersion remained around 0.9 ps^2 ± 0.1 ps^2, due to the unavoidable changes to the cavity length when the optical fibers are fusion spliced several times. Finally, when the effect of dispersion was studied, the net (normal) dispersion changed between 0.107 ps^2 and 0.254 ps^2. On the other hand, the power loses during each round trip of the light pulses are not significant, which is one of the main advantages of a full in-fiber configuration. From left to right −see Fig. 1(a), the discrete power loses are: −1 dB (80% reflectivity dichroic mirror), −0.7 dB (insertion loss of PM WDM), −0.9 dB (insertion loss of PM OFC), −0.1 dB (SESAM) and −0.97 dB (80% output of PM OFC); this is below 3.7 dB during each (half) round-trip. Additionally, it

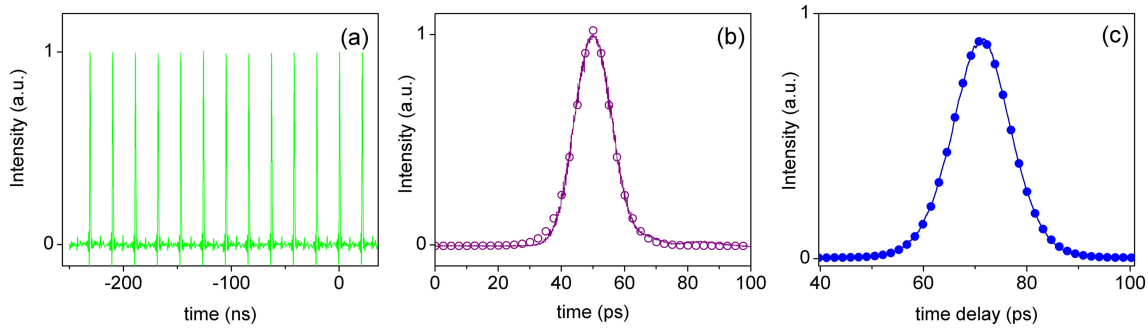

Fig. 2. (a) Real-time oscilloscope trace of the output light train. (b) Sampling oscilloscope trace of one single pulse and its corresponding fitting by a sech^2 profile (solid curve and open scatter, respectively). (c) Intensity autocorrelation trace (solid line) and its corresponding fitting by assuming a sech^2 profile for the waveform shown in (b) (open scatter points).

should be taken into account the output through the PM ISO, which is outside the resonant cavity, but it is an integral component of this laser, with a -1.5 dB of insertion loss. Additionally, some experiments were performed propagating the output light pulses of this laser by a PM PCF, whose measured transmission attenuation $\leq$0.12 dB/m. However, the fusion-splicing of a PM PCF with a standard PM SMF (in this case PM980-XP by Nufern), it is not a trivial task, due to the inherent numerical aperture mismatch. Thus, the measured power loss of the fusion-splicing between the PM SMF to the PM PCF was usually of -1.5 dB. Finally, the output light pulses were monitored by using: 60 GHz sampling oscilloscope provided with a fast built-in photodetector (53 GHz), real-time 2.5 GHz bandwidth oscilloscope, intensity autocorrelator (maximum scan range 200 ps), and an optical spectrum analyzer (wavelength accuracy $>$20 pm).

3. Results and Discussions

In the following, we will show first the characteristics of this all-normal-dispersion polarization-maintaining mode-locked fiber laser in the original configuration. Next, we will study the changes in the output light pulse train of this laser when the PM YDF length is varied, with the purpose to find the shortest pulse achievable in this configuration. Finally, we perform a similar analysis but now with a fixed PM YDF length and changing the net dispersion within the cavity.

3.1 Analysis of the Original Configuration

The laser was self-starting for all configurations once the pump power reaches the required level being unnecessary any mechanical perturbation to initiate mode-locking. In each case, we monitored the pulse waveform, spectrum, and intensity autocorrelation trace. We start our analysis by the original configuration; consisting of 0.39 m length of PM YDF and the rest of PM SMF, resulting in a round-trip cavity length of 4.23 m. Figure 2(a) shows the output light pulses train at a frequency of 48.54 MHz for a pump power of 101 mW. This laser operates at the fundamental frequency with one single pulse by round-trip time; as expected, the measured frequency corresponds well with the reciprocal of the round-trip time for the measured round-trip cavity length. In Fig. 2(b) we show the sampling oscilloscope trace, the output light pulses have a duration of $\sim$13 ps (which however should be taken as an approximate measurement, since it is at the limit of resolution of our tandem oscilloscope-photodetector). In the same figure, it is also shown a secant hyperbolic (sech^2) profile, only for comparison purposes. The output light pulse train of this laser showed good stability for all the series of experiments performed in this work, once the appropriate pump power range was found. In this specific case, the measured timing jitter was $\leq$722 fs and the standard deviation in intensity was $\leq$1.3%. In Fig. 2(c) it is shown the measured temporal intensity autocorrelation trace. It is known that the intensity autocorrelation

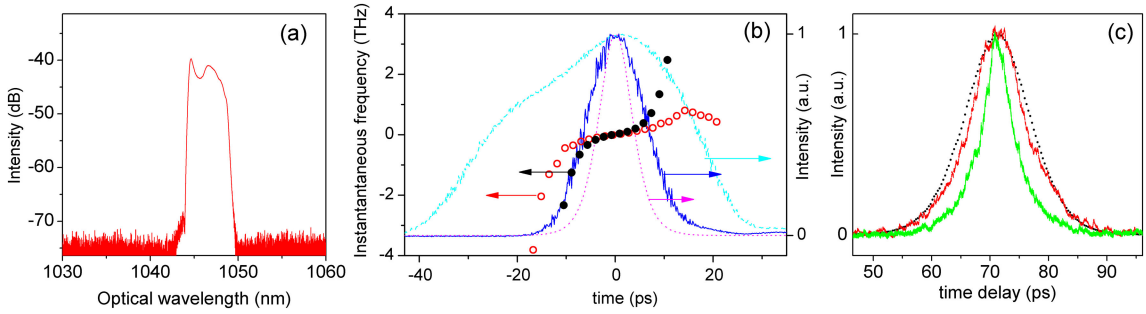

Fig. 3. (a) Output light pulse spectrum. (b) Left axis: instantaneous frequency profiles retrieved using as input pulse the measured light pulse and a simulated sech^2 profile with a FWHM of 8 ps (solid and open scatter points, respectively); Right axis: sampling oscilloscope traces of the input and output waveforms (solid blue and cyan curves, respectively) of the auxiliary dispersive delay line used to obtain the instantaneous frequency profile; together with a simulated sech^2 profile (dashed purple curve) (FWHM of 8 ps). (c) Measured intensity autocorrelation traces at the input of the PCF line (solid scatter points), and after one single PM PCF pass (red curve), and double PM PCF pass (green curve).

$A^{(2)}(t) = \int_{-\infty}^{\infty} d\tau I(\tau) I(\tau - t)$, of a Gaussian pulse $I(t) = \exp[-(2\ln 2t/T)^2]$, is another Gaussian function $A_G^{(2)}(t) = \exp[-(2\ln 2t/T')^2]$, where T and T' are the full-width at half maximum in the intensity profiles of pulse and autocorrelation traces, respectively, with $T' \cong 1.41T$. However, the intensity autocorrelation of a sech^2 profile $I(t) = \text{sech}^2(1.763t/T)$ is not simply another sech^2 profile, but $A_{\text{sech}^2}^{(2)}(t) = 3\text{cosech}^2(2.72t/T')[(2.72t/T')\coth(2.72t/T') - 1]$, with $T' \cong 1.54T$. We have contemplated both possibilities when the autocorrelation traces were fitted; i.e., $A_G^{(2)}(t)$ and $A_{\text{sech}^2}^{(2)}(t)$, and we have found that the later provides by far the best results, given a reduced chi-squared fitting one order of magnitude lower, as compared with the former. Figure 2(c) shows the fitting of the measured autocorrelation trace by $A_{\text{sech}^2}^{(2)}(t)$, confirming the good matching; from this measurement, we can reasonably affirm that the output light pulses of this mode-locked laser have a sech^2 profile with pulse duration of 8.3 ps. Finally, the spectrum of the output light pulses is shown in Fig. 3(a); without any filtering within the cavity, the laser emits at the central optical wavelength of 1046.8 nm (mean between the spectral positions of both edges of the steeped spectral profile), with a -3 dB bandwidth of 3.1 nm, and a -10 dB bandwidth of 5.9 nm. On the other hand, since the cavity is entirely ANDi, this laser operates at the dissipative soliton regime, as confirmed by the steep spectral edges in the optical spectrum. The time-bandwidth product (TBP) ranges between 7 and 13, showing that the mode-locked pulses are chirped, which also is a typical signature of the dissipative soliton regime.

Next, we measured the instantaneous frequency (IF) profile of the output light pulses by using a simple technique previously developed by us [20] and successfully applied since [21], [22]. The technique only requires the measurement of the temporal intensity waveforms at the input and output of the dispersive line together with the knowledge of the chromatic dispersion of the optical fiber; then the IF profile is obtained just by using a single equation in a non-iterative single-step numerical calculation which is shown in Figure 3(b). It is worthwhile to point out that this technique is particularly well suited for relatively long pulses, whose temporal intensity waveforms can be accurately recorded through an oscilloscope. In our experiments, however, this situation was clearly fulfilled at the dispersive line output, but only partially fulfilled at the input, where according to the autocorrelation measurements the pulse duration is slightly below the resolution limit of our oscilloscope, see Fig. 2(c). That is why we decide to make a further test, by replacing in the IF calculus the input pulse by a sech^2 profile with an FWHM of 8 ps, which is in accordance with the autocorrelation measurement, see Fig. 3(b). In both cases, we can observe approximate the same linear chirp with a slope of 33 GHz/ps at the central section of the light pulse $-$in the same order of magnitude than previously reported works [9], [11], [13], followed by an exponentially varying chirp much more abrupt in the extinction of the falling edge. This could be responsible for the lack

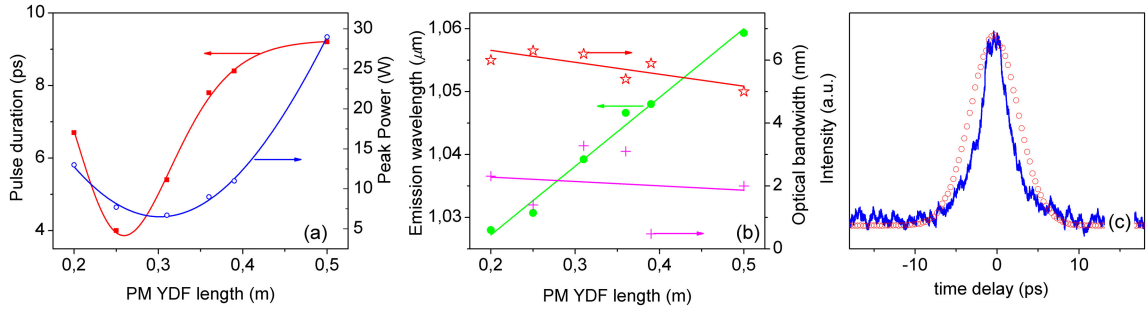

Fig. 4. (a) Pulse duration and peak power (left and right ordinates axis, respectively) as a function of the PM YDF length. (b) Central optical wavelength (left ordinate axis) and −3 dB/−10 dB bandwidths (right ordinate axis) as a function of the PM YDF length (solid crosses and open scatter stars, respectively). In all cases the solid curves are just a guide to the eyes. (c) Intensity autocorrelation trace at the output of the fiber laser—for a PM YDF length of 0.25 m—and after a single pass transmission through the PM PCF (open scatter points and solid curve, respectively).

of symmetry on the propagated waveform, see Fig. 3(b). Further, mode-coupling to the transversal polarization is not responsible for this asymmetry on the propagated pulse, since the fiber used (PM 980 XP by Nufern) has a strong anisotropy, with a beat length between 1.5 mm and 2.7 mm. Since the propagation length is 180 m, the other peak would be correspondingly located between 230 ps and 414 ps away from the main peak. This was experimentally corroborated by us, being the measured orthogonal peak at 265 ps, with −25 dB.

On the other hand, it is well known that DSs can be recompressed out of the cavity, by further propagation through a dispersive (anomalous) line. With this purpose, we disposed of a 26 m long PM PCF with either a single, or double-pass transmission possibilities, see Fig. 1(b); where a transversal scanning electronic microscope image of the PM PCF used is also shown in an inset of the same figure. The PM PCF has a chromatic dispersion of 17 ps/(nm km) at 1030 nm; therefore a single or double-pass transmission involves respectively -0.364 ps^2, and -0.728 ps^2 of chromatic dispersion. Figure 3(c) exemplifies the recompression possibilities for the output light pulses of this laser; to this end, it is showcased simultaneously the intensity autocorrelation traces of the input light pulse, single, and double-pass transmission through the PM PCF line. Therefore an input light pulse with a temporal duration of 8.2 ps is successively narrowed to 5.3 ps, and 3.1 ps after a single and double-pass transmission through the PM PCF delay line. Since the TBP of these pulses ranges between 7 and 13—and assuming enough anomalous dispersion—we envisage the limit for recompression of these pulses would be between 190 fs and 360 fs. However it is also fair to mention that this potential limit for recompression supposes an exactly linear chirp through the whole temporal waveform, neglecting the influence of the exponentially varying chirp at both edges that we have shown in Fig. 3(b).

3.2 Influence of the PM YDF Length on the Pulse Duration

We next analyzed the influence of the PM YDF length on the pulse duration taking as a reference the cavity studied above with a PM YDF length of 0.39 m. However, we always tried to minimize the inherent cavity length variations by adding/subtracting a small length of PM SMF, since both have a similar dispersion parameter. Therefore, the net (normal) dispersion remained relatively fixed in the range 0.9 ps^2 $\pm$ 0.1 ps^2 throughout this experiment, although the PM YDF length was changed from 0.13 m to 0.5 m. Figure 4(a) shows both the pulse duration and pulse peak power as a function of the PM YDF length. When the PM YDF length is reduced from 0.39 m, the pulse durations reduces too; however there is an optimum PM YDF length of 0.25 m, where the pulse duration is shortened down to 4 ps, further shortening of the PM YDF length down to 0.2 m increases again the pulse duration up to 6.7 ps. There is no possible further decreasing in the PM YDF length since no self-starting mode-locking was observed below 0.2 m of PM YDF length at the available pump power

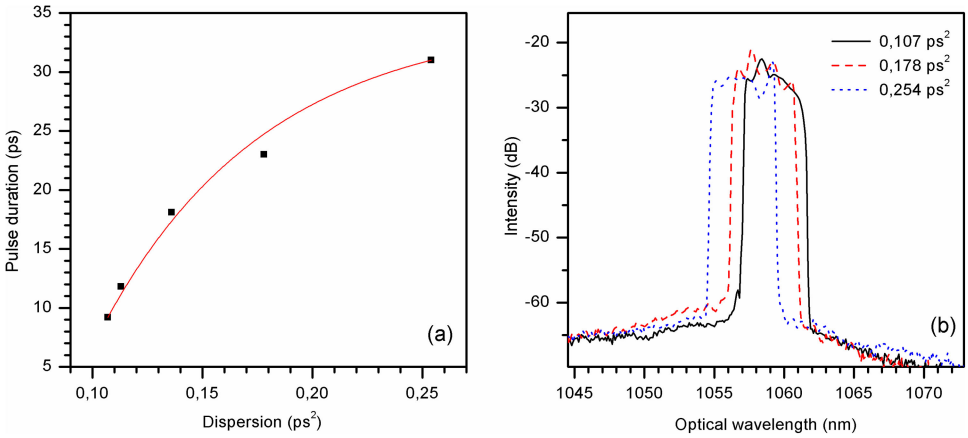

Fig. 5. (a) Pulse duration as a function of cavity dispersion, the solid curves are just a guide to the eyes. (b) Optical spectra for three different values of net cavity dispersion.

range. On the other direction, when the PM YDF is lengthened, the pulse duration also increases. As regards peak power, see the right axis in Fig. 4(a), it follows a similar trend as compared to the pulse duration, ranging from 7 W to 29 W; Whereas the peak power increment at 0.2 m of PM YDF length (before no self-starting mode-locking) is surely connected with the fact that the necessary pump power to reach a stable operation at this short YDF length was higher than at its nearest neighbor's operation points.

The characteristics steep spectral edges were preserved as the PM YDF length changes. However, there is a redshift of the optical central wavelength as the PM YDF length increases; see Fig. 4(b), which has been reported before in ANDi lasers [23]. This phenomenon is caused by the reabsorption mechanism of the YDF [24]. The −3 dB bandwidth does not show a clear trend; perhaps due to the presence of one peak generally closer to the short-wavelength edge. The characterization of a spectral profile through a –3 dB bandwidth is best suited for Gaussian spectra. However, it can be very inaccurate in the presence of peak oscillations, plus the characteristics steep spectral edges of dissipative solitons. For this reason, we have decided to include also the edge-to-edge optical bandwidth, which is generally used to provide a fairer estimation of the spectral characteristics of ANDi lasers [12], [23], in this case, through the −10 dB bandwidth. In this case, there is a slight narrowing in the optical bandwidth as the PM YDF is lengthened.

At last, we also tested the possibility to recompress the shortest pulses obtained from the oscillator when the PM YDF length was changed; i.e., 4 ps of pulse duration for 0.25 m of PM YDF length, see Fig. 4(a). Figure 4(c) shows the autocorrelation traces at the input and output of the 26 m long PM PCF—see Fig. 1(b). Since the PM PCF has a chromatic dispersion of 17 ps/(nm km) at 1030 nm; a single pass transmission involves −0.364 ps^2 of chromatic dispersion. Therefore, after a single-pass transmission through the PM PCF delay line, an input light pulse with a temporal duration of 4 ps is narrowed down to 2.5 ps. Unfortunately, the combination of a lower peak pulse power and higher transmission losses through the setup shown in Fig. 1(b) precluded the autocorrelation trace measurement of a double-pass transmission through the PM PCF, which would compress further this light pulse. However, since the TBP of this pulse ranges between 2 and 7, we envisage a potential limit for recompression of these light pulses between 200 fs and 900 fs (assuming an exactly linear chirp through the whole temporal waveform).

3.3 Influence of the Net-Normal Dispersion on the Pulse Duration

Finally, we progressively lengthened the optical fiber cavity with PM SMF, with the purpose to analyze the effects of the net dispersion on the emission of this laser, but always maintaining a fixed PM YDF length of 0.5 m. Therefore, the values of the net (normal) dispersion in the cavity

were: 0.107 ps^2, 0.113 ps^2, 0.136 ps^2, 0.178 ps^2, 0.254 ps^2, and 5 ps^2. Figure 5(a) shows the pulse duration as a function of dispersion. It can be observed, that the pulse duration monotonically increases with the chromatic dispersion; this result is in accordance with Ref. [11]. However, when the dispersion is raised too much—up to 5 ps^2—there is not mode-lock, showcasing the importance of dispersion management for stable dissipative soliton formation. On the other hand, we show in Fig. 5(b) the optical spectra corresponding to the net (normal) cavity dispersions: 0.107 ps^2, 0.178 ps^2, and 0.254 ps^2. We observed a redshift in the central optical wavelength as the dispersion decreases, whereas the edge-to-edge bandwidth remains practically unchanged.

4. Conclusions

We investigated an all-normal-dispersion in-fiber passively mode-locked Fabry-Pérot ytterbium-doped laser, and its subsequent pulse compression using a fabricated on purpose anomalous PM PCF. As opposed to previous setups; here the filtering action is solely performed by the finite bandwidth of the medium gain. Thanks to an all polarization-maintaining design, the laser is environmentally robust and insensitive against temperature variations and mechanical vibrations. The laser generates 8 ps width pulses at 1046.8 nm with a −10 dB bandwidth of 5.9 nm; which after recompression have a pulse duration of 3 ps (constrained by the value of available anomalous dispersion). Additionally, we found an optimal medium gain length where the oscillator produces the shortest light pulses (4 ps for a PM YDF length of 0.25 m), which can be further recompressed down to 2.5 ps (constrained by both the value of available anomalous dispersion and peak power). On the other hand, we also found that the shortest pulses are obtained when the net-normal cavity dispersion decreases. Thus, combining a PM cavity, adjusting properly the active fiber length and the overall normal dispersion, and using pulse compression with an anomalous PM PCF, it should be possible to produce all-fiber environmentally stable femtosecond light pulses.

References

[1] L. F. Mollenauer and R. H. Stolen, "The soliton laser," *Opt. Lett.*, vol. 9, pp. 13–15, 1984.
[2] H. Haus and M. Islam, "Theory of the soliton laser," *IEEE J. Quantum Electron.*, vol. 21, no. 8, pp. 1172–1188, Aug. 1985.
[3] P. Grelu and N. Akhmediev, "Dissipative solitons for mode-locked lasers," *Nature Photon.*, vol. 6, pp. 84–92, 2012.
[4] A. Chong, J. Buckley, W. Renninger, and F. Wise, "All-normal-dispersion femtosecond fiber laser," *Opt. Exp.*, vol. 14, pp. 10095–10100, 2006.
[5] A. Chong, W. H. Renninger, and F. W. Wise, "All-normal-dispersion femtosecond fiber laser with pulse energy above 20 nJ," *Opt. Lett.*, vol. 32, pp. 2408–2410, 2007.
[6] D. Mortag, D. Wandt, U. Morgner, D. Kracht, and J. Neumann, "Sub-80-fs pulses from an all-fiber-integrated dissipative-soliton laser at 1 μm," *Opt. Exp.*, vol. 19, pp. 546–551, 2011.
[7] D. S. Kharenko, E. V. Podivilov, A. A. Apolonski, and S. A. Babin, "20 nJ 200 fs all-fiber highly chirped dissipative soliton oscillator," *Opt. Lett.*, vol. 37, pp. 4104–4106, 2012.
[8] M. Brotons-Gisbert *et al.*, "Comprehensive theoretical and experimental study of short- and long-term stability in a passively mode-locked solitonic fiber laser," *J. Lightw. Technol.*, vol. 33, no. 19, pp. 4039–4049, Oct. 2015.
[9] C. Aguergaray, R. Hawker, A. F. J. Runge, M. Erkintalo, and N. G. R. Broderick, "120 fs, 4.2 nJ pulses from an all-normal-dispersion, polarization-maintaining, fiber laser," *Appl. Phys. Lett.*, vol. 103, 2013, Art. no. 121111.
[10] J.-B. Lecourt, C. Duterte, F. Narbonneau, D. Kinet, Y. Hernandez, and D. Giannone, "All-normal dispersion, all-fibered PM laser mode-locked by SESAM," *Opt. Exp.*, vol. 20, pp. 11918–11923, 2012.
[11] M. Erkintalo, C. Aguergaray, A. Runge, and N. G. R. Broderick, "Environmentally stable all-PM all-fiber giant chirp oscillator," *Opt. Exp.*, vol. 20, pp. 22669–22674, 2012.
[12] B. Ortaç, M. Plötner, J. Limpert, and A. Tünnermann, "Self-starting passively mode-locked chirped-pulse fiber laser," *Opt. Exp.*, vol. 15, pp. 16794–16799, 2007.
[13] C. Aguergaray, N. G. R. Broderick, M. Erkintalo, J. S. Y. Chen, and V. Kruglov, "Mode-locked femtosecond all-normal all-PM Yb-doped fiber laser using a nonlinear amplifying loop mirror," *Opt. Exp.*, vol. 20, pp. 10545–10551, 2012.
[14] Y. Yu *et al.*, "Highly-stable mode-locked PM Yb-fiber laser with 10 nJ in 93-fs at 6 MHz using NALM," *Opt. Exp.*, vol. 26, pp. 10428–10434, 2018.
[15] B. Xu, A. Martinez, S. Y. Set, and S. Yamashita, "All-polarization maintaining fiber laser and pulse compressor," *IEEE Photon. Technol. Lett.*, vol. 30, no. 24, pp. 2151–2154, Dec. 2018.
[16] X.-S. Xiao, "Low-repetition-rate, all-polarization-maintaining Yb-doped fiber laser mode-locked by a semiconductor saturable absorber," *Chin. Phys. B*, vol. 26, 2017, Art. no. 114204.
[17] X. Shen, W. Li, and H. Zenga, "Polarized dissipative solitons in all-polarization-maintained fiber laser with long-term stable self-started mode-locking," *Appl. Phys. Lett.*, vol. 105, 2014, Art. no. 101109.

[18] A. Chong, W. H. Renninger, and F. W. Wise, "Properties of normal-dispersion femtosecond fiber lasers," *J. Opt. Soc. Amer. B*, vol. 25, pp. 140–148, 2008.
[19] R. I. Woodward *et al*., "Scalar nanosecond pulse generation in a nanotube mode-locked environmentally stable fiber laser," *IEEE Photon. Technol. Lett*., vol. 26, no. 16, pp. 1672–1675, Aug. 2014.
[20] C. Cuadrado-Laborde, A. Carrascosa, P. Pérez-Millán, A. Díez, J. L. Cruz, and M. V. Andrés, "Phase recovery by using optical fiber dispersion," *Opt. Lett*., vol. 39, pp. 598–601, 2014.
[21] C. Cuadrado-Laborde, M. Brotons-Gisbert, G. Serafino, A. Bogoni, P. Pérez-Millán, and M. V. Andrés, "Phase recovery by using optical fiber dispersion and pulse pre-stretching," *Appl. Phys. B*, vol. 117, pp. 1173–1181, 2014.
[22] C. Cuadrado-Laborde, I. Armas-Rivera, A. Carrascosa, E. A. Kuzin, A. Díez, and M. V. Andrés, "Instantaneous frequency measurement of dissipative soliton resonance light pulses," *Opt. Lett*., vol. 41, pp. 5704–5707, 2016.
[23] X. Xiao, Y. Hua, B. Fu, and C. Yang, "Experimental investigation of the wavelength tunability in all-normal-dispersion ytterbium-doped mode-locked fiber lasers," *IEEE Photon. J*., vol. 5, no. 6, Dec. 2013, Art. no. 1502807.
[24] L. A. Gomes, L. Orsila, T. Jouhti, and O. G. Okhotnikov, "Picosecond SESAM-based ytterbium mode-locked fiber lasers," *IEEE J. Sel. Top. Quant*., vol. 10, no. 1, pp. 129–136, Jan./Feb. 2004.